ARTICLE IN PRESS
RSE-07910; No of Pages 11
Remote Sensing of Environment xxx (2011) xxx–xxx
Contents lists available at ScienceDirect
Remote Sensing of Environment
journal homepage: www.elsevier.com/locate/rse

Sensitivity of SAR data to post-fire forest regrowth in Mediterranean and boreal forests

Mihai Tanase [a,*], Juan de la Riva [a], Maurizio Santoro [b], Fernando Pérez-Cabello [a], Eric Kasischke [c]

[a] University of Zaragoza, Pedro Cerbuna 12, 50009, Zaragoza, Spain
[b] Gamma Remote Sensing, Worbstrasse 225, CH-3073 Gümligen, Switzerland
[c] University of Maryland, 2181 LeFrack Hall, College Park, MD 20742, USA

ARTICLE INFO

Article history:
Received 22 June 2010
Received in revised form 23 March 2011
Accepted 2 April 2011
Available online xxxx

Keywords:
Forest regrowth
Backscatter
Interferometric coherence
X-, C- and L-band SAR

ABSTRACT

Disturbed forests may need decades to reach a mature stage and optically-based vegetation indices are usually poorly suited for monitoring purposes due to the rapid saturation of the signal with increasing canopy cover. Spaceborne synthetic aperture radar (SAR) data provide an alternate monitoring approach since the backscattered microwave energy is sensitive to the vegetation structure. Images from two regions in Spain and Alaska were used to analyze SAR metrics (cross-polarized backscatter and co-polarized interferometric coherence) from regrowing forests previously affected by fire. TerraSAR-X X-band backscatter showed the lowest sensitivity to forest regrowth, with the average backscatter increasing by 1–2 dB between the most recent fire scar and the unburned forest. Increased sensitivity (around 3–4 dB) was observed for C-band Envisat Advanced Synthetic Aperture (ASAR) backscatter. The Advanced Land Observing Satellite (ALOS) Phased Array-type L-band Synthetic Aperture Radar (PALSAR) L-band backscatter presented the highest dynamic range from unburned to recently burned forests (approximately 8 dB). The interferometric coherence showed low sensitivity to forest regrowth at all SAR frequencies. For Mediterranean forests, five phases of forest regrowth were discerned whereas for boreal forest, up to four different regrowth phases could be discerned with L-band SAR data. In comparison, the Normalized Difference Vegetation Index (NDVI) provided reliable differentiation only for the most recent development stages. The results obtained were consistent in both environments.

1. Introduction

Information on forest regrowth is of great interest for scientists and land managers dealing with environmental issues (e.g., climate impact, carbon budget, forest management, etc.) since forests need a long time to reach the biomass level, structure and carbon sink capacity prior to disturbance. Satellite remote sensors provide the ability to collect recurrent data facilitating the temporal analysis of wide areas. Changes in forest structure and composition (caused by fires, floods, winds etc.) and subsequent processes may be identified and monitored by means of remote sensing using optical (Marchetti et al., 1995; Patterson & Yool, 1998; Viedma et al., 1997), radar (Bourgeau-Chavez et al., 1997, 2002; Ruecker & Siegert, 2000; Siegert & Ruecker, 2000) or lidar (Goetz et al., 2010) sensors. Suitability of remote sensing data for monitoring vegetation recovery is determined by two factors: a) sensitivity to alterations in the radiometric response because of the vegetation development and b) the spatial resolution of satellite imagery which allows the characterization of the response patterns.

Disappearance of immediate disturbance effects (e.g. charcoal-ash remains), increase of vegetation and the subsequent decrease of bare soil cover are targets for remote sensing satellites operating in the visible and infrared region of the electromagnetic spectrum. In consequence of such dynamics, infrared reflectance increases and red and blue reflectance decreases caused by changes in chlorophyll levels as a result of recovery from disturbance are detected by optical sensors. A number of studies evidenced this as useful for vegetation monitoring (Díaz-Delgado & Pons, 2001; Henry & Hope, 1998; Pérez-Cabello, 2002). The Normalized Difference Vegetation Index (NDVI) (Rouse et al., 1973) has been the most frequently used tool for monitoring, analyzing, and mapping temporal and spatial vegetation variations (Díaz-Delgado et al., 2002, 2003; Viedma et al., 1997). However, NDVI responds more to changes in leaf area than to changes in overall biomass (Henry & Hope, 1998) and its relation to leaf area index (LAI) varies both intra- and inter-annually reaching saturation levels at LAI values that reach a maximum prior to point where an ecosystem fully recovers from disturbance (Wang et al., 2005). Therefore, tracking vegetation development using NDVI is usually limited to the first decade after disturbance. For example, the analysis of fire-affected oak forests in NE Spain showed that pre-fire NDVI values were reached after only 7 years (Díaz-Delgado & Pons, 2001). Similar trends were found by (Clemente

* Corresponding author. Tel.: +34 976 762 060; fax: +34 976 761 506.
E-mail address: mihai.tanase@tma.ro (M. Tanase).

0034-4257/$ – see front matter © 2011 Elsevier Inc. All rights reserved.
doi:10.1016/j.rse.2011.04.009

et al., 2009; Vila & Barbosa, 2010) in other Mediterranean regions whereas in boreal forests pre-fire NDVI values were reached after 13 years (Cuevas-Gonzalez et al., 2009).

Forests may need decades to reach the mature stage and the short period within which optical based vegetation indices reach pre-disturbance levels implies limited value for longer-term monitoring. SAR data have the potential to significantly extend the monitoring period since the backscattered signal is directly influenced by the forest structure. The signal backscattered from forests is the result of complex interactions between microwave electromagnetic energy and the ground and vegetation scattering components (Richards et al., 1987). It depends on the amount and geometric properties of vegetation on site as well as soil dielectric and geometric (roughness) properties on one hand (M. Dobson et al., 1992; Imhoff, 1995) and on the radar frequency, polarization and look direction on the other hand (Imhoff, 1995). X-band waves mostly interact with leaves/needles, twigs and small branches, C-band waves with leaves and small and secondary branches whereas L-band waves interact mostly with primary braches and tree trunks (Toan et al., 1992). Backscatter sensitivity to forest structural parameters increases with wavelength of the microwave sensor being used. Typically, the backscatter coefficient, i.e. the backscattered intensity per unit area, increases with forest biomass reaching saturation as a function of forest type and structure. Higher sensitivity to forest regrowth was reported for L-band (23 cm wavelength) HH polarization compared to C-band (6 cm wavelength) VV polarization for a 10 year old burn in China (Sun et al., 2002). The longer L-band wavelength allowed the differentiation among young (i.e. regrowth) and mature forest stands. In a Mediterranean environment temporal changes in forest biomass were assessed using multi-temporal C-band VV polarized images in order to characterize vegetation recovery processes (Minchella et al., 2009). Furthermore, interferometric coherence, i.e. a measure of the correlation of the coherent signal recorded by the radar at two different polarizations and/or times, could provide additional information for monitoring affected areas. Repeat-pass interferometric coherence computed from images acquired with a certain temporal separation is usually low over mature forests and is significantly higher for areas covered by short vegetation or bare soil (Wegmuller & Werner, 1995). In forests affected by fire, C- and L-band co-polarized coherence was found to be higher than in undisturbed areas (Liew et al., 1999; Takeuchi & Yamada, 2002).

In previous articles (Tanase et al., 2009, 2010a, 2010b), we have analyzed the signatures of SAR backscatter and interferometric coherence with respect to burn severity. Increasing burn severity implies a reduction of the number of scatterers in the canopy layer, leading to increased penetration of microwaves through the canopy and larger proportion of the ground component to the total backscatter. Burn severity and forest regrowth are different aspects of post-fire processes. The first one is considered a first-order fire effect (e.g. fuel consumption, plant injury and death, greenhouse gasses emission etc.) while the second is a second-order effect which may be evident many decades after fire. When relating SAR metrics to forest age after fire, one should bear in mind that the scattering scenario is different. At the start of the regrowth, the scattering originates from the forest floor, which is covered by shrubs and herbs. When the regrowth advances, the backscattered signal is the sum of a component due to the live vegetation and a component due to the forest floor, which can be different depending on the environmental conditions.

Previous studies on post-fire forest monitoring carried out using SAR data could not take advantage of the cross-polarized backscatter, which is more sensitive to forest structure than the co-polarized backscatter (M.C. Dobson et al., 1992; Rignot et al., 1994; Toan et al., 1992), nor evaluated the sensitivity of backscatter and coherence at different wavelengths to forest regrowth. Cross-polarized data could provide better differentiation between recovery stages. This paper aims at filling this gap by reporting on X-, C- and L-band cross-polarized backscatter and co-polarized interferometric coherence from fire disturbed areas to assess the utility of these metrics for forest regrowth monitoring in ecosystems common to the Mediterranean basin. In addition, regrowth in boreal forests affected by fire was studied using L-band data. Although the radar dataset also included co-polarized backscatter and cross-polarized coherence measurements, it was decided to focus on the metrics that presented the largest sensitivity to forest structural properties. The sensitivity of SAR measurements to regrowth was compared to trends in NDVI obtained from visible and near infrared sensor data acquired over the study sites.

Forest regrowth is here quantified in terms of the number of years since disturbance (ysd). Throughout this paper we considered the terms “forest age” and “years since disturbance (ysd)” as interchangeable since the first seedlings appear during the following spring after the fire event.

2. Study regions

Two regions located in the Mediterranean and the boreal zones were used. The first region (Zuera) was located in the central Ebro valley, northeastern Spain and has a Mediterranean climate with continental features and marked seasonal variation of precipitations. This region is characterized by a hilly relief, with elevation ranging between 400 m and 750 m above sea level. The topography is moderate, around 65% of the surface presenting slopes smaller than 15°. Aleppo pine forests (*Pinus halepensis* P. Mill.) cover approximately 22,000 ha being interspersed with shrub vegetation and cereal crops. The forest has a homogeneous structure. The average height is approximately 6.5 m and the average biomass around 45 t/ha. Old stands reach heights of 12–13 m and 90 t/ha (Notivol et al., 2005). During the last century the region has been repeatedly affected by fires, with some areas having been burned up to three times. Fourteen sites affected by fire were identified using Landsat MSS and TM imagery which was also used for digitizing the fire perimeters. The year of burn as observed from the satellite images was cross-checked with information obtained from the Regional Environmental Service of Aragón, which also provided the perimeters of the older burns in this region (1922 and 1952). The year of burn and the affected area are presented in Table 1. Aleppo pine regenerates quickly after fire due to the large seed bank stored in the canopy (Tapias et al., 2001) and the relatively young age (15 years) at which it reaches sexual maturity. Post-fire succession in aleppo pine forests involves stand self-replacement (Buhk et al., 2006) (e.g., shrubs dominated by *Quercus coccifera* L. and immature pines followed by mature pine forest with a dense understory layer). In areas repeatedly affected by fire the vegetation is dominated by shrub species and the succession to forest needs considerably longer time. Previous studies suggested no clear relationship between seedling density and burn severity; however, seedling growth was higher in areas affected by high burn severities (Pausas et al., 2002). The minimum human intervention and the vigorous forest growth at Zuera sites due to the specific microclimate of the area and the resilience of aleppo pine forest provided ideal conditions for the forest regeneration.

The boreal region used in this study was located near Delta Junction, in interior Alaska. In this region, the average annual temperature is −2.1 °C, with the warmest month being July (15.6 °C) and the coldest January (−19.7 °C). Average annual precipitation is 290 mm, with three-quarters of this amount occurring during the growing season (May to September) (Kasischke et al., 2002). Twenty sites affected by fire were identified using fire perimeter information provided by the Alaska Interagency Coordination Center (Table 1). The sites were mostly located on a gently sloping alluvial outwash plane north of the Alaska Range, with elevations ranging between 300 and 600 m, and slopes being less than 3°. A detailed description of the region can be found in (Kasischke & Johnstone, 2005). The upland forests at the Alaskan sites are undergoing secondary succession following fires, where poorly drained soils are occupied by black spruce (*Picea mariana* P. Mill). on

Table 1
Surface of the fire-affected areas computed from the digitized fire perimeters. Years since disturbance is referred to the SAR dataset acquisition (see Table 3).

Zuera sites			Delta Junction sites		
Burn year	Affected area (ha)	Years since disturbance (ysd)	Burn year	Affected area (ha)	Years since disturbance (ysd)
1922	1030	87	1947*	2097	60
1952*	2000	57	1951	9387	56
1970*	272	39	1954	7312	53
1979	680	30	1969*	28101	38
1983	25	26	1969	892	38
1984	29	25	1971*	2150	36
1985	10	24	1979*	13588	28
1986*	303	23	1979	2518	28
1990	23	19	1979	1342	28
1994	37	15	1980	3338	27
1994	96	15	1981	8269	26
1995*	3100	14	1984	1233	23
2001*	26	8	1987*	18336	20
2005	30	4	1993*	192	14
2006*	31	3	1994	318	13
2008*	2200	<1	1994*	8904	13
			1995	951	12
			1998*	22045	9
			1999*	7581	8
			2001	44.7	6

* Analyzed sites.

cooler, wetter sites and white spruce (*Picea glauca* (Moench) Voss.) on warmer drier sites (Viereck et al., 1983). Post-fire succession in black spruce forests involves self replacement (e.g., shrubs to immature spruce/shrub mixture followed by mature forests), while relay floristics occur after fire on sites occupied by white spruce forests (shrubs following by *Populus* sp. or *Betula* sp. forests followed by mixed deciduous/spruce forests followed by mature white spruce forests).

3. Earth observation and ancillary data

For the Zuera region, the SAR dataset consisted of images acquired by the TerraSAR-X (TSX), Environmental Satellite (Envisat) Advanced SAR (ASAR) and Advanced Land Observing Satellite (ALOS) Phased Array-type L-band SAR (PALSAR) sensors. For the Delta Junction region, only ALOS PALSAR data were available. Table 2 presents the acquisition dates together with the main characteristics of the datasets. TerraSAR-X dual-polarized images were acquired in strip map mode (SM). One Envisat ASAR image was acquired in Alternating Polarization mode (AP) with HH and HV polarizations whereas the two images used for interferometric processing were acquired in Image Mode (IM). ALOS PALSAR data were acquired in full polarimetric (PLR) and dual polarization Fine Beam Dual (FBD) modes. For the Zuera site, backscatter measurements were available for similar incidence angles for all sensors whereas the incidence angle of the image pairs used for interferometric coherence analysis varied between 23° (ASAR) and 40° (TSX).

The SAR data for the Zuera sites were absolutely calibrated, multi-looked to obtain the desired 25 m spatial resolution and geocoded to Universal Transverse Mercator (UTM) projection using a 20 m spatial resolution digital elevation model (DEM). The DEM was obtained from the regional government of Aragón. Topographic normalization of the backscatter to account for the effect of varying incidence angle from near to far range and the effective pixel area was applied (Ulander, 1996). The resulting images were in gamma nought (γ°) format, and only included variations of the scattering properties of a target due to local orientation. Generation of the SAR coherence signatures involved co-registration of the images, spatial multi-looking, common band filtering and differential interferogram computation, coherence estimation, and geocoding to UTM projection. Detailed description of the processing is given in (Tanase et al., 2010b, 2010c).

The PALSAR dataset (FBD mode) for the Delta Junction sites was processed in a similar way. The images were geocoded to 30 m using a 60 m spatial resolution DEM and UTM projection. The National Elevation Dataset (NED) from US Geological Survey (USGS) was used. Although most of the area presented flat or nearly flat topography, normalization of the backscatter was applied in order to obtain similar metrics (γ°) as for the Zuera sites.

Fig. 1 shows the coherence image product (red: coherence; green: backscatter, blue: backscatter ratio) for the ALOS PALSAR FBD image pairs. Fire perimeters together with the burn year were superimposed over the satellite images. The coherence image product shows the burned sites in red and orange because of overall high coherence and low backscatter. Forests appear in green tones (high backscatter and low coherence) at Delta Junction whereas at Zuera they appear in yellow tones (high backscatter and high coherence). The large difference in forest coherence values for the two regions was explained by the more stable weather conditions at the Zuera sites and the greater stiffness of the L-band scatterers in Mediterranean pine forests. Red colors correspond to sparsely vegetated areas which did not change (high coherence and low backscatter) whereas blue colors represent areas of considerable backscatter change between image acquisitions.

For each region, a Landsat image acquired on 22 August 2008 (Zuera) and 12 August 2009 (Delta Junction) was used to estimate the NDVI in the studies sites. The Landsat images were transformed to the same coordinate system used to geocode the SAR data. Both images underwent radiometric corrections to compensate for variations in sensor radiometric response, sun angle, sun azimuth and topography. Raw digital number (DN) values were converted to satellite reflectance.

To aid the interpretation, meteorological data collected from the nearest available meteorological station were used. For the Zuera region, temperature measurements were available from the Casa Perez station located at approximately 10 km west of the study area whereas

Table 2
SAR acquisition date, incidence angle, perpendicular baseline (Pb), temporal baseline (Tb), and meteorological conditions at acquisition: maximum temperature (Tmax) and minimum temperature (Tmin) in °C and the accumulated precipitations (AcPp) in mm.

Area	Sensor	Polarization	Incidence angle	Acquisition date 1	Acquisition date 2	Pb (m)	Tb (days)	AcPp date1	Tmax date1	Tmin date1	AcPp date2	Tmax date2	Tmin date2
Zuera	Backscatter analysis												
	TSX	HH,HV	25°	2008.12.24				0	−3	−6			
	ASAR	HH,HV	23°	2009.03.19				0	20	−1			
	PALSAR	All	25°	2009.04.28				3.5*	18	10			
	PALSAR	HH,HV	34°	2009.08.20				0	34	15			
	Interferometric coherence analysis												
	TSX	HH,HV	40°	2008.11.16	2008.12.19	231	33	0	14	−2	0	11	4
	ASAR	HH	23°	2009.01.08	2009.02.12	34	35	0.5	0	−6	0.5	10	4
	PALSAR	HH,HV	34°	2009.08.20	2009.10.05	508	46	0	34	15	0	26	11
Delta Junction	Backscatter and interferometric coherence analysis												
	PALSAR	HH,HV	34°	2007.08.15	2007.09.30	483	46	1.3*	24	12	0.1	9	−3

* Precipitations registered partially during the day of SAR acquisition.

Please cite this article as: Tanase, M., et al., Sensitivity of SAR data to post-fire forest regrowth in Mediterranean and boreal forests, *Remote Sensing of Environment* (2011), doi:10.1016/j.rse.2011.04.009

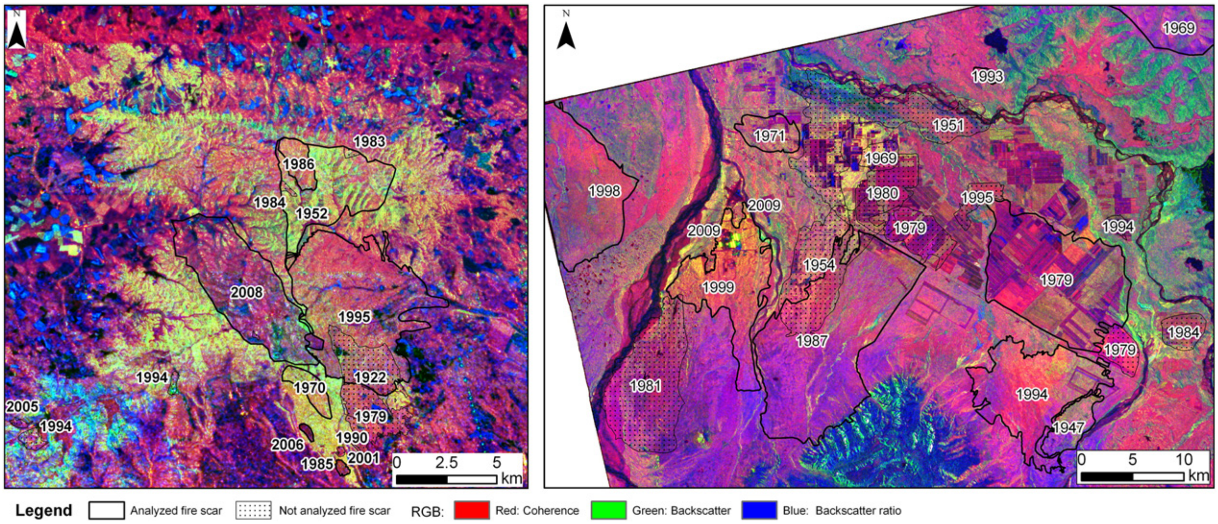

Fig. 1. Disturbed areas as revealed by ALOS PALSAR data at Zuera (left) and Delta Junction (right) sites. False color composite of (red) HH coherence, (green) HH backscatter and (blue) HH backscatter ratio. (For interpretation of the references to colour in this figure, the reader is referred to the web version of this article.)

precipitation data were obtained from an automatic rain gauge installed roughly at the center of the study area. For the Alaskan region meteorological data were available from the Delta Junction station located 45 km to the west of the study area (see Table 2). Accumulated precipitation (AcPp) in mm was computed taking into account the last 5 days before acquisition of SAR data. At the Zuera region, all images were acquired under dry conditions except the full polarimetric ALOS PALSAR dataset (28 April 2009), as shown in Table 2. At Delta Junction site a previous study (Kasischke et al., 2011) had examined the precipitation patterns for the two ALOS PALSAR scenes used for this study and concluded that the soil moisture, based on the previous 60 days precipitations, was high during the 15 August 2008 collection and very high during the 30 September 2008 collection. While Kasischke et al. (2011) concluded that temporal differences in soil moisture could contribute to variations in PALSAR SAR backscatter in forests with low biomass, they also concluded that these variations were most pronounced when comparing sites with very high soil moisture. The average L-band backscatter for the low biomass sites studied by Kasischke et al. (2011) in the Delta Junction region were only slightly different for the 15 August and 30 September 2008 PALSAR data collections, and there were significant correlations between aboveground biomass and backscatter on both dates.

4. Methods

The lack of long-term systematically archived SAR data for most of the SAR frequencies conditioned the analysis. Therefore, we carried out the assessment of microwave backscatter sensitivity to forest regrowth using single date imagery and areas affected by fire in different years. The forest age interpreted as years since disturbance (ysd) was used as a quantitative parameter since it is strongly related to forest structure properties (e.g. biomass, tree height, basal area etc.) The small study areas offered relatively homogeneous forest conditions and the single date image minimized possible spatial heterogeneities of soil moisture or canopy moisture content.

Five regrowth sites (i.e. fire scars) larger than 250 ha were the main focus of the study at Zuera. In addition, two smaller sites (burns from 2001 and 2006) were included (for signature analysis) to cover the last decade. For the Delta Junction region, nine sites were selected for the analysis (Table 1). The selection was carried out taking into account site size, vegetation type (scrublands, open forests and woody wetlands were eliminated), fire recurrence (sites repeatedly affected by fire were eliminated), availability of larger burns from the same year, obvious human related land cover changes and availability of the SAR data at all frequencies (Zuera sites only).

To reduce pixel wise noise of backscatter and coherence measurements, the analysis was conducted on samples produced by averaging over several pixel values. The larger sites and the rather flat topography at Delta Junction allowed the generation of contiguous plots (1 ha) using a systematic grid spaced at 600 m. For the Zuera sites, the study was carried out using a set of random plots, so called pseudo-plots. Pseudo-plots were generated by averaging inside each site random pixels of similar slope and aspect with respect to the radar viewing geometry. The generation of pseudo-plots was considered due to the rough topography in most of the studied sites. To avoid bias related to size, only pseudo-plots containing a constant number of pixels were considered. Nine pixel per pseudo-plot (0.55 ha) appeared to be optimal for the selected spatial resolution (25 m) of the geocoded images (Tanase et al., 2009).

For the Mediterranean sites, a threshold on NDVI was used to eliminate non-forest pixels thus assuring pseudo-plots homogeneity. For the Delta Junction region, plots with large difference (>0.15) between maximum and minimum NDVI pixel values were discarded due to the increased probability of containing different land cover types. In total 652 plots were analyzed at Delta Junction (15 to 250 depending on the site size) whereas around 2700 pseudo-plots where analyzed at Zuera, depending on image coverage. Changes in local topography greatly influenced the radar signal when analyzing burn severity levels (Tanase et al., 2010b, 2010c). Therefore, for the Zuera sites the pseudo-plots were clustered into 5°-wide intervals of local incidence angle (Tanase et al., 2010a) with 15 to 100 pseudo-plots available for the analysis at each site and incidence angle interval. For the small sized sites (i.e. 2001 and 2006), the total number of pseudo-plots was small, i.e. between 10 and 25. Since these sites were located on rather flat terrain, most of the pseudo-plots belonged only to one or two local incidence angle intervals.

To provide a reference on the forest regrowth status, the Mediterranean sites were visited near the time of SAR image acquisitions. Since vegetation conditions inside each site were rather homogeneous, two to three points per burn scar were used for the assessment of vegetation cover fraction and the average tree height and diameter. The cover fraction of the vegetation layers was visually estimated at each plot on a 15 m radius. For trees taller than 2 m, the diameter (D) was measured at breast height whereas for the smaller trees the diameter was measured at half of their height. Vegetation layers present at Zuera sites consisted of herbs and low shrubs less than 1 m tall for the most recent burns, shrubs and small trees up to 5 m tall, and trees up to 15 m tall for

Please cite this article as: Tanase, M., et al., Sensitivity of SAR data to post-fire forest regrowth in Mediterranean and boreal forests, *Remote Sensing of Environment* (2011), doi:10.1016/j.rse.2011.04.009

Table 3
Average vegetation conditions for the analyzed fire scars at Zuera sites.

Site	Strata	Cover (%)	Height (m)	D (cm)
Undisturbed	Herbs	20–70	0.3–1	
	Shrubs	5–60	0.5–2	8–35
	Trees	40–75	8–12	
57 ysd	Herbs	10	0.2–0.3	
	Shrubs	20–25	0.7–1.5	10–25
	Trees	60–75	8–9	
39 ysd	Herbs	10–20	0.1–0.3	
	Shrubs	50–60	0.5–2	9–16
	Trees	90	3–6	
23 ysd	Herbs	10	0.4	
	Shrubs	5–10	0.5–1	3–5
	Trees	70–80	1.5–4	
14 ysd	Herbs	10	0.2–0.3	
	Shrubs	30–35	0.5–1	2–3
	Trees	55–65	0.7–2	
8 ysd	Herbs	80	0.2–1	
	Shrubs	10	0.5–1	<3
	Trees	5–10	0.5–1	
3 ysd	Herbs	70	50–80	
	Shrubs	5	0.5–0.8	<1
	Trees	N/A	0.1–0.2	
<1 ysd	Herbs	5–20	0.1–0.3	
	Shrubs	5–20	0.1–0.3	8–35
	Trees	N/A	8–12	

the oldest burns. A short description of the average vegetation status at each site is presented in Table 3 whereas Fig. 2 illustrates vegetation regrowth phases found at some of the assessed points. No field data were available for Delta Junction sites. Post-fire vegetation is shown in Fig. 3 for three of the analyzed sites.

Descriptive statistics were used to analyze backscatter and coherence sensitivity to forest age. Analysis of variance (ANOVA) was used to assess the possibility to discern between forest recovery stages using mean values of SAR backscatter and coherence, for sites larger than 200 ha. Pair-wise comparison using Games–Howell test (Games & Howel, 1976) provided information on the significantly different mean values. This test was used because it does not assume equal variances, the sample size were unequal and the homogeneity of variance assumption was violated in the ANOVA analysis. The smaller sites (i.e. less than 200 ha) were not included in the analysis due to the small number of samples.

5. Results and discussion

Recent studies by Kasischke et al. (2011) showed that variations in soil moisture over time influenced the relationships between L-band SAR backscatter and biomass in many of the Alaskan sites used in this study. Therefore, variations in soil moisture should be considered when using SAR backscatter data to assess patterns of post-fire recovery. If all the sites being analyzed are contained within a single SAR scene, then steps should be taken to account for between-site variations in soil drainage. Both regions used in this study had sites with similar soil types, so between-site variations in soil moisture were not an important factor in contributing to variations in backscatter using data collected on the same date.

5.1. Signature analysis

Similarly to the analysis carried out in (Tanase et al., 2010b) when relating burn severity to SAR backscatter, we observed strong sensitivity of the regrowth in terms of local orientation of the forest with respect to the SAR look direction. In Fig. 4, we show plots of mean backscatter (HV polarization) as a function of the local incidence angle and forest age for each SAR frequency for the Zuera sites. Flat areas correspond to local incidence angles around 25°. Slopes oriented towards the sensor correspond to local incidence angles between 5° and 25° whereas slopes oriented away from the sensor correspond to local incidence angles between 25° and 55°. The average backscatter of the small sites is represented by the filled symbols whereas the average backscatter of undisturbed forests (NB) is represented by the grey circles. The standard error of the mean is given in Table 4 for some of the local incidence angle intervals.

Regardless of the incidence angle, HV-polarized backscatter increased with increasing forest age because increased vegetation cover increased the volume scattering component. The dynamic range of the X-band backscatter from unburned to recently burned forest was low (1–2 dB in flat areas) and decreased to 1 dB for the largest incidence angles. Stronger sensitivity to changes in forest structure was observed at C-band. The dynamic range between unburned forest and the most recent burn was relatively constant over the entire range of incidence angles reaching around 3 dB (Fig. 4b). Generally, the X- and C-band backscatter difference between undisturbed forest and different stages of forest regrowth was low except for the most recent

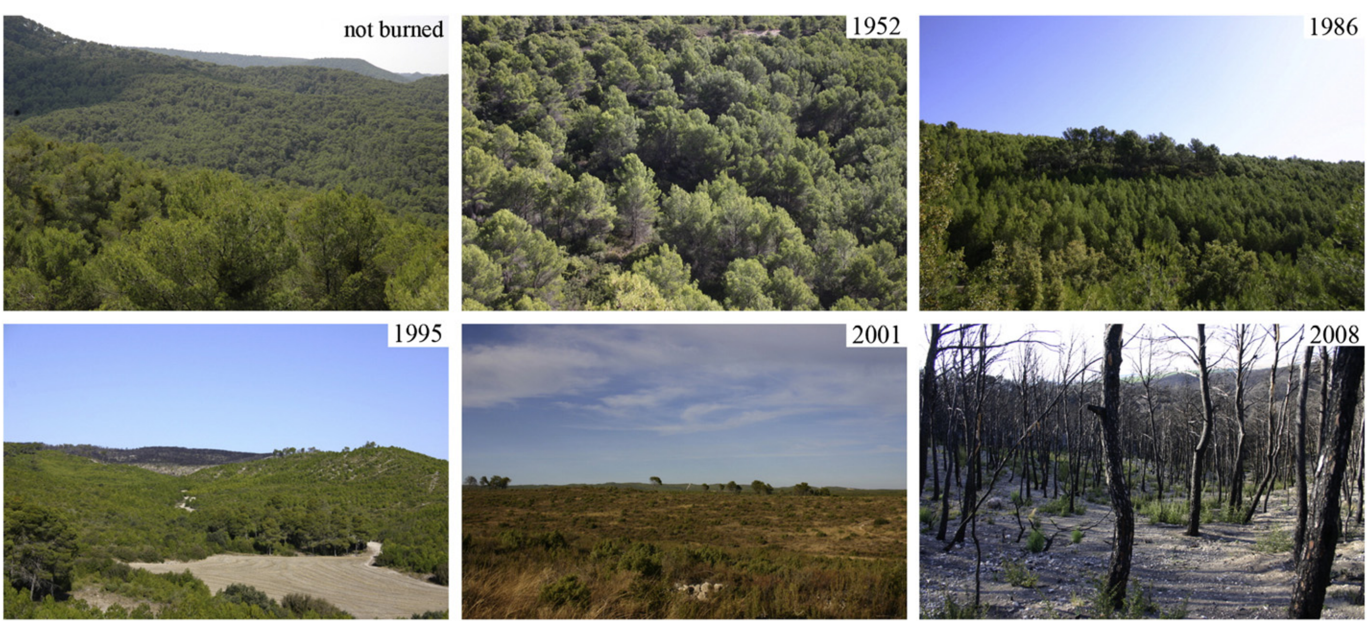

Fig. 2. Examples of vegetation condition at the Zuera sites. The pictures were taken during summer 2009.

Please cite this article as: Tanase, M., et al., Sensitivity of SAR data to post-fire forest regrowth in Mediterranean and boreal forests, *Remote Sensing of Environment* (2011), doi:10.1016/j.rse.2011.04.009

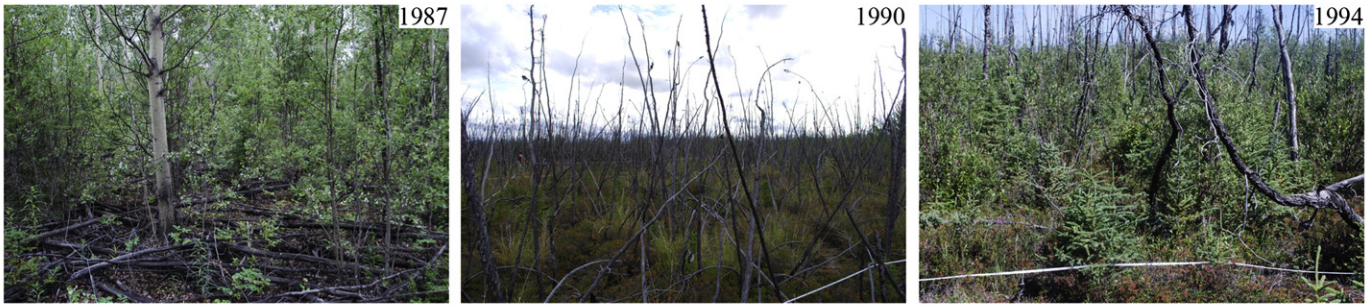

Fig. 3. Examples of vegetation condition at the Delta Junction sites. The pictures were taken during summer 2008.

affected sites (one to seven years since disturbance) where the regrowth was negligible. The greatest difference (around 7 dB) of the backscatter coefficient between forest regrowth stages was observed at L-band. Fig. 4c illustrates L-band average backscatter of the PLR data (2009.04.28) since it was acquired at similar incidence angle as for X-

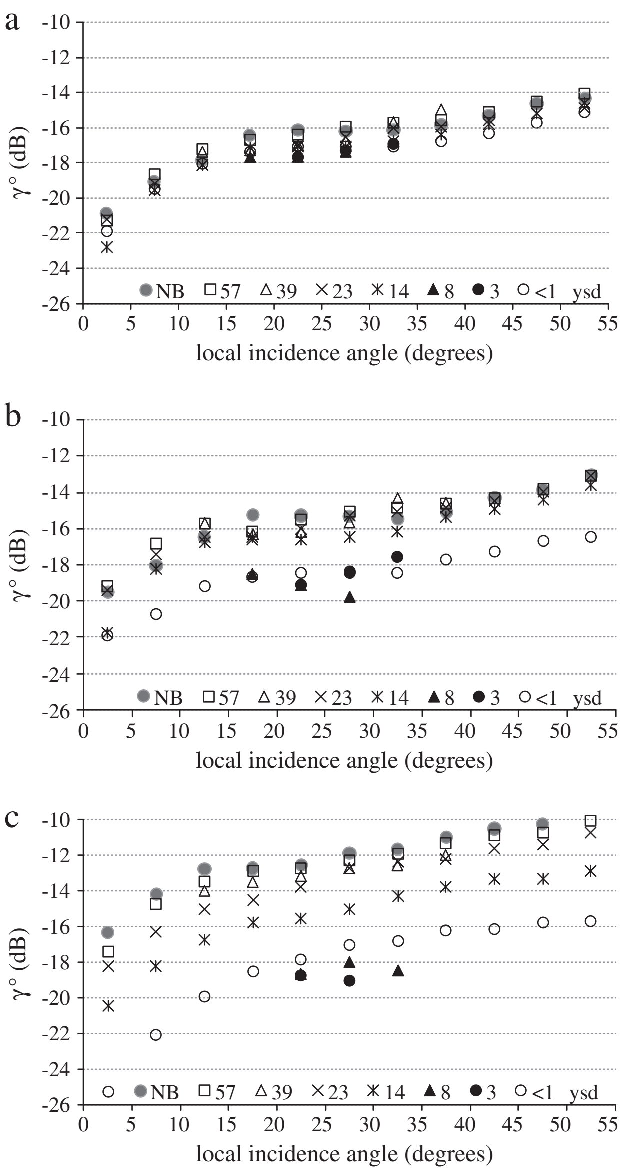

Fig. 4. Cross-polarized (HV) normalized backscatter coefficient (γ°) trend as a function of the local incidence angle and the year since disturbance (ysd) for the Zuera sites: (a) X-band data from 24 December 2008; (b) C-band data from 19 March 2009; and (c) L-band data from 28 April 2009.

and C-band. The PALSAR image was however acquired during precipitations, which influenced the backscattering coefficient reducing the dynamic range from old to young forests (see also Fig. 5). Burned trees still present on site (<1 ysd site) increased C- and L-band cross-polarized backscatter when compared to 3 and 8 ysd sites from which the dead trees had been removed before the acquisition of the Envisat ASAR image.

Fig. 5 illustrates the HV backscatter as a function of the forest age for the Zuera and Delta Junction regions, for PALSAR FBD data acquired at 34.3° look angle. Because of the flat topography at Delta Junction, the analysis is focused only on flat terrain. Horizontal lines represent the average backscatter of undisturbed areas. The trends of the mean backscatter values were similar. The only obvious difference is represented by the lower backscatter values observed at Zuera during the first years after the fire, which was explained by the different type of post-fire management. The Spanish administration usually removes the burned standing trees after fire whereas in boreal forest trees are left at on site. Thus, the backscatter from burned areas in the boreal zone contains a significant component due to the remaining vegetation whereas in Mediterranean burns this component is usually missing. This explanation was supported by the backscatter levels observed for the <1 ysd Zuera site where trees had not been removed before image acquisition. In such case, the backscatter values were closer to the values observed at Delta Junction. At the Zuera sites increased dynamic range (10 dB) was observed for the FBD data acquired under dry conditions when compared to PLR data, which had been acquired during rainfall. The larger dynamic range could be also the consequence of the shallower look direction of the FBD mode with respect to the PLR mode.

In a similar manner to Fig. 4, Fig. 6 illustrates co-polarized (HH) coherence trends for the Zuera sites. Regardless of the range of local incidence angles, lower coherence was observed with increasing forest age at X- and C-band. The standard error of the mean is given in Table 4. The highest coherence values were recorded for the most recent burns which presented little or no vegetation cover. It is interesting to note that the presence of burned standing trees on the <1 ysd site was sufficient to cause decorrelation of the signal almost completely at X-band (Fig. 7a). At L-band, the coherence showed a completely opposite trend (Fig. 7c). High coherence was observed for older burns while for the most recent fires the coherence was significantly lower (see also Fig. 8). At the time of acquisition of the PALSAR data, the environmental conditions had been dry for a long period, which may have caused the upper part of the canopy to be rather transparent to the impinging L-band microwaves. Furthermore, Mediterranean pines are stiff trees so that typical decorrelating agents in forests (wind and moisture changes) are not playing a significant role and the coherence is preserved. Yet unclear is the low coherence of recent fires which were characterized primarily by shrub vegetation. Changes in soil moisture between the two image acquisitions (46 days) can be considered a plausible explanation; nonetheless, we did not have direct evidence of this. The decreasing trend of coherence with local incidence angle was observed at all

Table 4
Average properties of the analyzed sites for different slope orientations. Data represent mean values and the standard error of the mean. Different letters indicate statistically significant differences between sites (p<0.05). Zuera.

	Slope orientation	Undisturbed	57 ysd	39 ysd	23 ysd	14 ysd	<1 ysd
Backscatter							
X-band	Toward sensor	−19.1 (0.36) a	−18.7 (0.25) a	N/A	−19.2 (0.18) a	−19.6 (0.22) a	−19.5 (0.21) a
HV	Flat area	−16.2 (0.06) a	−15.9 (0.11) a	−16.8 (0.05) bc	−16.6 (0.11) b	−17.1 (0.10) cd	−17.1 (0.06) d
	Away from sensor	−14.6 (0.04) a	−14.5 (0.05) a	N/A	−15.2 (0.05) b	−15.2 (0.06) b	−15.7 (0.05) c
C-band	Toward sensor	−18.0 (0.27) a	−16.8 (0.20) b	N/A	−17.4(0.22) ab	−18.2 (0.22) a	−20.7 (0.20) c
HV	Flat area	−15.3 (0.14) a	−15.5 (0.24) ab	−16.2 (0.11) bc	−16.0 (0.14) b	−16.6 (0.15) c	−18.4 (0.16) d
	Away from sensor	−15.1 (0.14) ab	−14.6 (0.15) a	N/A	−14.8(0.15) ab	−15.3 (0.12) b	−17.7 (0.12) c
L-band	Toward sensor	−16.9 (0.09) a	−18.3 (0.15) b	N/A	−19.8 (0.13) c	−21.7 (0.12) d	−25.0 (0.14) e
HV*	Flat area	−15.0 (0.05) a	−15.8 (0.07) b	−15.8 (0.04) b	−17.0 (0.09) c	−18.7 (0.10) d	−21.8 (0.16) e
	Away from sensor	−13.3 (0.05) a	−14.0 (0.08) b	N/A	−15.0 (0.12) c	−16.9 (0.10) d	−20.9 (0.20) e
Coherence							
X-band	Toward sensor	0.17 (0.00) a	0.19 (0.00) b	N/A	0.27 (0.01) c	0.33 (0.00) d	0.34 (0.00) d
HH	Flat area	0.18 (0.00) a	0.15 (0.00) b	0.22 (0.00) c	0.23 (0.01) c	0.33 (0.01) d	0.31 (0.00) d
	Away from sensor	0.11 (0.00) a	0.10 (0.00) a	N/A	0.13 (0.00) b	0.24 (0.00) c	0.22 (0.00) d
C-band	Toward sensor	0.21 (0.01) a	0.22 (0.01) a	N/A	0.21 (0.00) a	0.28 (0.01) b	0.53 (0.01) c
HH	Flat area	0.18 (0.00) a	0.20 (0.00) b	0.18 (0.00) a	0.19 (0.01) ab	0.28 (0.01) c	0.38 (0.01) d
	Away from sensor	0.12 (0.00) a	0.14 (0.00) a	N/A	0.16 (0.00) b	0.19 (0.00) c	0.24 (0.01) d
L-band	Toward sensor	0.77 (0.00) a	0.71 (0.01) b	N/A	0.83 (0.00) c	0.77 (0.00) a	0.72 (0.00) b
HH	Flat area	0.77 (0.00) a	0.78 (0.00) ab	0.79 (0.00) b	0.84 (0.00) c	0.76 (0.00) d	0.63 (0.00) e
	Away from sensor	0.76 (0.00) a	0.80 (0.00) b	N/A	0.83 (0.00) c	0.76 (0.00) a	0.56 (0.01) d

* Reported for data not affected by rain (FDB, 2008.08.20, look angle 34°).

frequencies especially for the most recently affected sites and was related to the smaller ground component for the slopes oriented away from the sensor.

At the Delta Junction sites, the L-band coherence decreased with increasing forest age due to the increased vegetation cover (Fig. 7). The coherence was lower overall because of the 46-day interval between acquisitions. In the boreal zone, the environmental conditions during summer months are prone to rapid changes which cause strong temporal decorrelation in interferograms spanning several weeks. Long periods of stable environmental conditions, as shown in this article for the Zuera site or in Thiel et al. (2009) for Siberian forest, instead preserve coherence.

5.2. Statistical analysis

The analysis of variance helped understanding the potential of SAR data to monitor forest regrowth status. For the Zuera sites, Table 4 illustrates backscatter and coherence response for three intervals of local incidence angle corresponding to the main type of relief orientation with respect to the radar viewing geometry: *i)* slopes tilted towards the sensor, *ii)* flat or nearly flat areas and *iii)* slopes tilted away from the sensor. The mean values and the standard error of the mean are presented for the large sites (>200 ha) at each SAR frequency. Due to the rather flat topography, the statistics for the area affected in 1970 (39 ysd) are presented only for the flat terrain class. For the Delta Junction sites, the analysis was carried out considering only the flat terrain conditions. The results from Delta Junction sites are presented in Table 5. Pair-wise comparison results were coded by letters. For sites sharing the same letter the average backscatter or coherence were not significantly different ($p<0.05$) meaning that it was not possible to statistically separate the respective regrowth phases. For simplicity in interpretation we considered similar regrowth phases when the difference in mean backscatter or interferometric coherence between sites was less than 1 dB and 0.1 U respectively. We judged a mean backscatter difference of less than 1 dB between two consecutive burns impractical for differentiation of the regrowth phase. The threshold was based on the highest standard error of the mean (see Tables 4 and 5) for a confidence interval of 99%. Residual speckle was negligible since the statistical analysis was carried out over several thousands of the original pixels (multi-look processing, pseudo-plot averaging and analysis at fire scar level). Therefore, it was reasonable to assume that the variability inside a given site corresponded mostly to differences in forest regrowth. Similar reasoning was applied for the coherence analysis.

The analysis of variance for the backscatter coefficient revealed statistically significant differences between different stages of forest regrowth for all frequencies and slope orientations at the Zuera sites (Table 4). However, the small dynamic range from undisturbed to recently disturbed sites observed at X-band HV polarization indicated limited practical use for regrowth phases discrimination. C-band data showed increased discrimination potential although only the most recently affected site (<1 ysd) was reliably differentiated for all slopes; the average backscatter difference with respect to older forests was between 1 and 2 dB. The largest number of forest regrowth phases was differentiated at L-band. Five groups were consistently separated for all slope orientations. Each individual site was separated with the exception of the two oldest ones (57 ysd and 39 ysd). The average backscatter difference between consecutive groups was larger than 1 dB.

Statistically significant differences were found between forest regrowth phases when analyzing the interferometric coherence at the

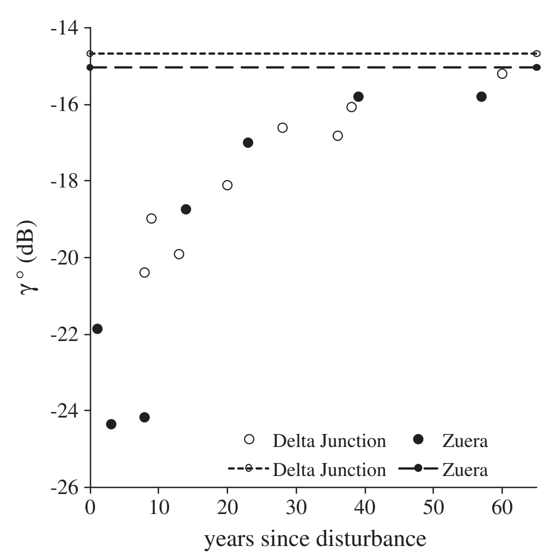

Fig. 5. Average L-band normalized HV backscatter coefficient (γ°) as a function of forest age for flat areas. Delta Junction (15 August 2007) and Zuera (20 August 2009) sites. Horizontal lines represent backscatter levels of undisturbed forests.

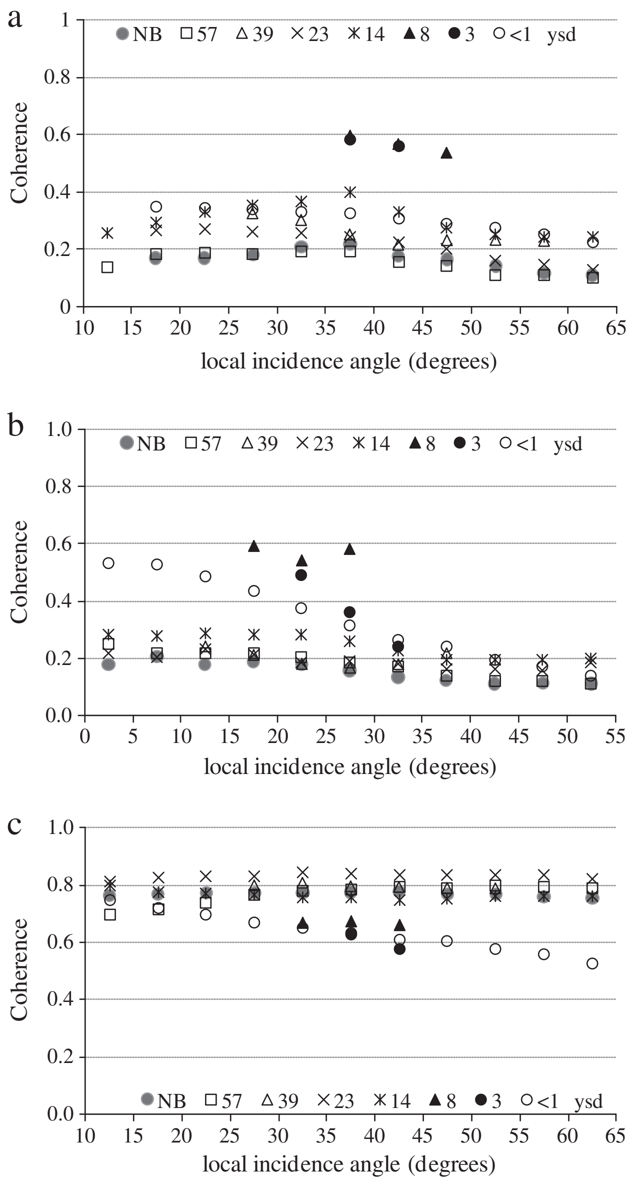

Fig. 6. Co-polarized (HH) coherence trend as a function of the local incidence angle and the year since disturbance (ysd). X-band 2008.11.16 / 2008.12.19 pair (a), C-band 2009.01.08/2009.02.12 pair (b) and L-band 2009.08.20/2009.10.05 pair (c). Zuera site.

Zuera sites. However, the small dynamic range (<0.2) did not allow reliable identification among different phases of forest regrowth at C- and L-band due to the small variation among individual sites (0.03–0.05). The only exception was the <1 ysd site where the forest floor provided a stable scattering scenario not greatly influenced by the remaining burned trees.

At the Delta Junction sites, the analysis of variance produced less obvious results due to smaller time interval between disturbance events, slower regrowth rates and larger variability of the boreal forest in terms of structure and species composition (Table 5). Thus, most of the sites pertained to at least two groups in the pair-wise comparison illustrating the transitional nature of the forest regrowth. Four regrowth phases could be differentiated at HV polarization using backscatter information: *i)* undisturbed forest and 60 ysd site, *ii)* 38 ysd, 36 ysd and 28 ysd sites, *iii)* 20 ysd site and iv), 13 ysd, 9 ysd and 8 ysd sites. These regrowth phases corresponded largely to the decade of disturbance suggesting temporally consistent traits. As for Zuera, the interferometric coherence showed low discrimination potential for forest regrowth monitoring.

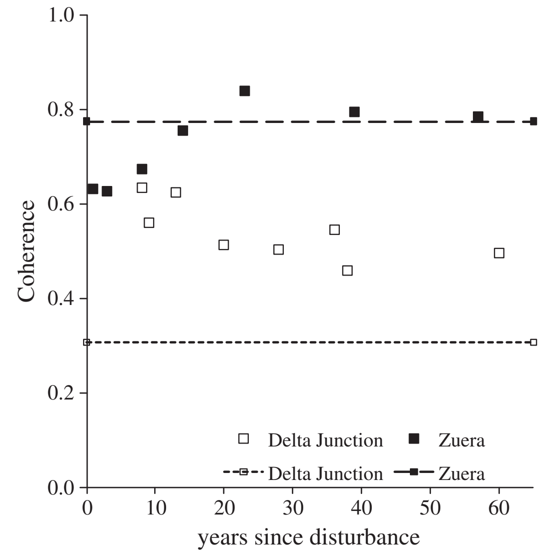

Fig. 7. Average L-band HH coherence as a function of forest age for flat areas. Delta Junction (2007.08.15/2007.09.30 pair) and Zuera (2009.08.20/2009.10.05 pair) sites. Horizontal lines represent coherence levels of undisturbed forests.

Statistically significant differences were found between sites but their use for operational application appears to be limited by the small variability of the coherence among individual sites. Only the undisturbed forests were reliably identified at HH polarization since their mean coherence was significantly lower.

5.3. Regrowth dynamics of SAR and optical data

To assess the capability of a remote sensing parameter to monitor forest regrowth, the relative difference of the remote sensing parameter (e.g. backscatter) of a fire-affected area with respect to the undisturbed conditions is here introduced. We will refer to this quantity as percentage of change.

$$\%_{change} = \frac{\bar{x}_{NB} - \bar{x}_{fire}}{\bar{x}_{NB}} * 100 \quad (1)$$

In Eq. (1), $\bar{x}_{NB}$ represents the value of the remote sensing parameter for undisturbed conditions whereas $\bar{x}_{fire}$ represents the corresponding value for a specific disturbed site. Since it was shown in this Section that the SAR parameter most sensitive to regrowth is L-band HV backscatter, the analysis will be focused on this parameter. As comparison, the percentage of change for the most widely used parameter for monitoring vegetation recovery, i.e. NDVI, is also considered.

The percentage of change with respect to the undisturbed forest is presented as a function of time from the disturbance for L-band HV backscatter and NDVI in Fig. 8. For clarity reasons, the two parameters are represented on opposite sides of the zero change line. The change in backscatter was computed using the average of the plots located in flat areas whereas for optical data all plots were used when averaging for a given site. Mature undisturbed forests were represented on the zero change line. For the Zuera sites, the average age of the forest (65 years) was used to estimate the fire-return interval. For interior Alaska the fire regime of black spruce dominated forests was previously estimated between 80 (Hu et al., 2006) and 120 (Kasischke et al., 2002) years. There is a certain lag between forest age at the Zuera and the Delta Junction sites due to the different date of the last burns.

Fig. 8 shows that the percentage of change for L-band HV backscatter and NDVI decreased with forest age during the first years. After a certain

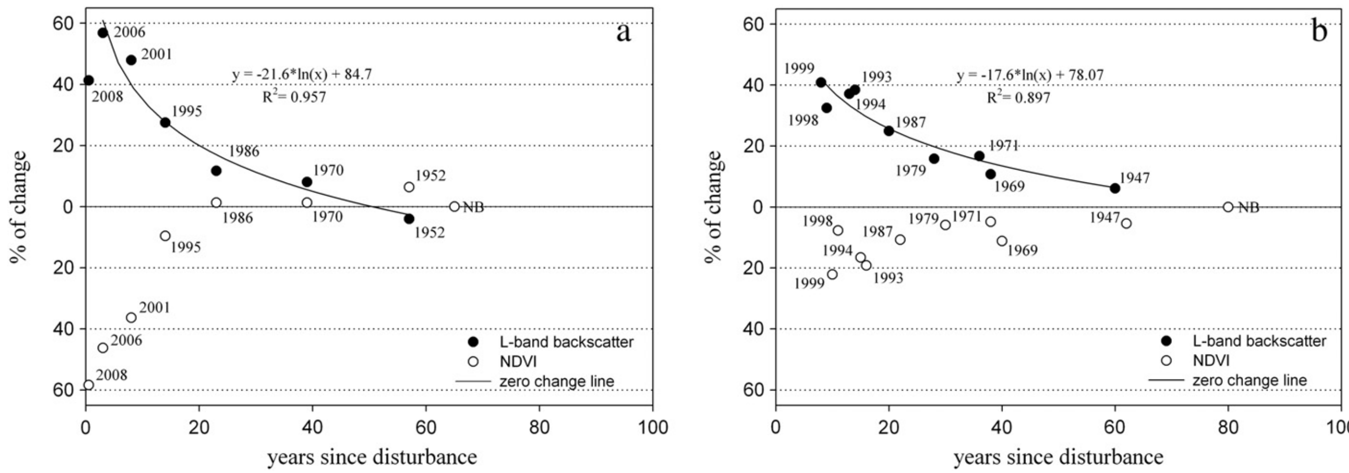

Fig. 8. Forest recovery as seen by L-band HV SAR and optical based NDVI—percentage of change with respect to the undisturbed area for Zuera (a) and Delta Junction (b) sites.

Table 5
Average properties of the analyzed sites. Data represent mean values and the standard error of the mean. Different letters indicate statistically significant differences between sites ($p<0.05$). Delta Junction.

	Undisturbed	60 ysd	38 ysd	36 ysd	28 ysd	20 ysd	13 ysd	9 ysd	8 ysd
Backscatter									
L-band HV	−14.7(0.37)a	−15.2(0.18)a	−16.1(0.37)ab	−16.8(0.31)bc	−16.6(0.14)b	−18.1(0.11)c	−19.9(0.17)d	−19.0(0.09)d	−20.4(0.17)e
Coherence									
L-band HH	0.31(0.02)a	0.49(0.02)b	0.46(0.03)bc	0.55(0.01)bc	0.50(0.01)b	0.51(0.00)b	0.62(0.01)d	0.56(0.01)c	0.63(0.01)d

age, the trend flattened out, indicating that the signal had reached values similar to those of mature forest. At Zuera, the loss of sensitivity of the NDVI metric occurred approximately 15 years after the disturbance. This loss corresponded to the increased canopy cover of the regenerating forest with the age (Table 3). The NDVI percentage of change becomes negligible when the forest canopy fraction reached relatively high levels (70–80% for the 20 ysd site). On the contrary, the L-band HV backscatter percentage of change reached the zero change line approximately 40 to 50 years after disturbance which is explained by the longer periods needed for the recovery of forest structure. The comparative analysis of Table 3 and Fig. 8 highlighted the correspondence between the evolution of the forest cover fraction and NDVI percentage of change on one hand and of the forest structural parameters (diameter and height) and L-band SAR percentage of change on the other hand. Similarly, for the boreal forests NDVI reached pre-disturbance values much sooner when compared to L-band cross-polarized backscatter which needed approximately 60 years. Fig. 8 also shows that the radar data were sensitive to the trees remaining on site. If burned trees are not removed, the backscatter from recently affected areas may be confused with forest regrowth especially during the first years (e.g. <1 ysd at Zuera).

To evaluate the association strength between forest age and the percentage of change with respect to undisturbed forest, a logarithmic model was fitted to the measurements (Fig. 8). The <1 ysd Zuera site was excluded since it represented an atypical phase which usually disappears past the second year after disturbance. For both regions, the percentage of change for the L-band HV backscatter showed similar trends, suggesting consistent behavior over different environments. Fig. 9 illustrates a comparison of the values predicted by the two logarithmic functions. As reference we considered the 1:1 line, indicating perfect correspondence between trends. Fig. 9 shows that regrowth trends are similar during the first years after fire (i.e. for the highest percentage of change). The slower growth rate of the boreal forest is revealed by the additional time needed to reach pre-fire forest structure when compared to Mediterranean forests. When the Mediterranean forest has reached the level of unburned forests (0% change), i.e. after 65 years, at Delta Junction the forest still needs to recover about 10% of the pre-fire structure.

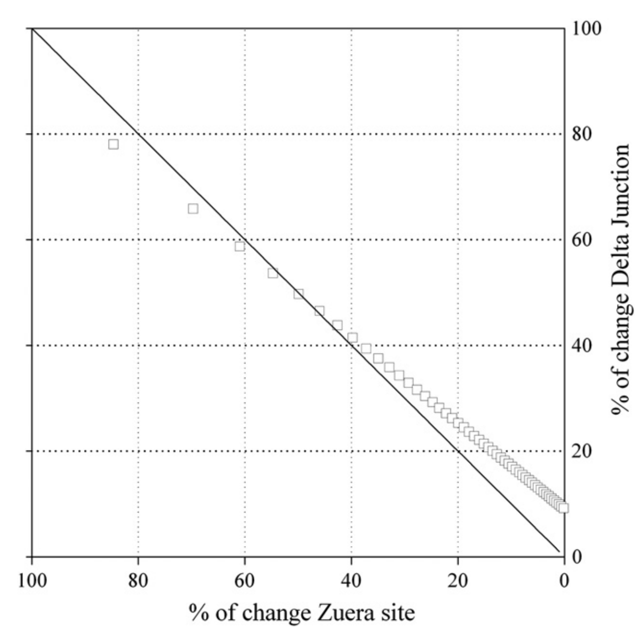

Fig. 9. Co-plotted model-based percentage of change with respect to undisturbed area for Zuera and Delta Junction regions.

6. Conclusions

The properties of multi-frequency SAR backscatter and interferometric coherence from Mediterranean and boreal disturbed forests were investigated with the aim of assessing the potential of active microwave remote sensing for forest regrowth monitoring. A comparison with NDVI was carried out to establish the advantages and limitations of SAR data compared to optical sensors. For Mediterranean forests, the L-band HV-polarized SAR backscatter allowed the best differentiation of regrowth phases (five phases for six dates) whereas at X- and C-band the HV-polarized backscatter was less sensitive to modification in forest structure due to the rapid saturation of the signal. For boreal forest four different regrowth phases were separated. Co-polarized repeat-pass coherence presented weak sensitivity to the different forest regrowth phases. Separation was possible only for the most recently affected sites (<15 ysd) regardless of the radar frequency.

Analysis of the NDVI in terms of percentage of change with respect to undisturbed forests in the case of Mediterranean pine forest showed saturation at about 10–20 years after disturbance provided that forest cover recovery is not hindered by other factors (e.g. recurrent fires). L-band SAR backscatter provided much larger monitoring intervals: around 45 years for Mediterranean and 60 years for boreal forests. Therefore, L-band SAR cross-polarized data appear more appropriate to differentiate among forest regrowth stages when compared to optical based indices. The usefulness of SAR data for regrowth monitoring is further supported by the independence from solar illumination and visibility. At high latitudes, the availability of usable optical images is scarce due to frequent clouds. Only six images with modest cloud cover were available for Delta Junction region during the vegetation season between 1999 and 2009 from which just one was cloud free over all burns. In addition, although only few images were analyzed, certain confidence in the consistency of the results is provided by the observations reported in Santoro et al. (2009), who showed that the seasonal variability of the L-band HV backscatter under unfrozen conditions is limited.

At the Zuera sites, the study took advantage of the vigorous forest growth which allowed almost ideal conditions for natural regeneration that could not be met in other regions. In addition, repeatedly burned areas could present different regeneration patterns especially when disturbances occur at short time intervals, before forests reach maturity. Therefore, the temporal recovery trend registered for the Zuera site could take longer in forests exposed to harsh environment or when disturbance cycle is short. The study assumed relatively homogenous soil moisture conditions due to the single date image approach used. As noted by Kasischke et al. (2011), analyzing SAR biomass-backscatter relationships using data collected on different dates will require development of approaches to account for variations in soil moisture.

Acknowledgments

This work has been financed by the Spanish Ministry of Science and Education and the European Social Fund: FPI grant BES-2006-11684 and projects CGL2005-04863 and CGL2008-01083. TerraSAR-X data were provided by Deutsches Zentrum für Luft- und Raumfahrt (DLR) in the framework of LAN0464 project. ASAR and PALSAR data were provided by European Space Agency (ESA) in the framework of C1P.5446 project and by the Americas ALOS Data Node.

References

Bourgeau-Chavez, L. L., Harrell, P. A., Kasischke, E. S., & French, N. H. F. (1997). The detection and mapping of Alaskan wildfires using a spaceborne imaging radar system. *International Journal of Remote Sensing*, *18*, 355–373.

Bourgeau-Chavez, L. L., Kasischke, E. S., Brunzell, S., & Mudd, J. P. (2002). Mapping fire scars in global boreal forests using imaging radar data. *International Journal of Remote Sensing*, *23*, 4211–4234.

Buhk, C., Götzenberger, L., Wesche, K., Gómez, P. S., & Hensen, I. (2006). Post-fire regeneration in a Mediterranean pine forest with historically low fire frequency. *Acta Oecologica*, *30*, 288–289.

Clemente, R. H., Cerrillo, R. M. N., & Gitas, I. Z. (2009). Monitoring post-fire regeneration in Mediterranean ecosystems by employing multitemporal satellite imagery. *International Journal of Wildland Fire*, *18*, 648–658.

Cuevas-Gonzalez, M., Gerard, F., Balzter, H., & Riaño, D. (2009). Analysing forest recovery after wildfire disturbance in boreal Siberia using remotely sensed vegetation indices. *Global Change Biology*, *15*, 561–577.

Díaz-Delgado, R., Lloret, F., & Pons, X. (2003). Influence of fire severity on plant regeneration by means of remote sensing imagery. *International Journal of Remote Sensing*, *24*, 1751–1763.

Díaz-Delgado, R., Lloret, F., Pons, X., & Terradas, J. (2002). Satellite evidence of decreasing resilience in Mediterranean plant communities after recurrent wildfires. *Ecology*, *83*, 2293–2303.

Díaz-Delgado, R., & Pons, X. (2001). Spatial patterns of forest fires in Catalonia (NE Spain) along the period 1975–1995. Analysis of vegetation recovery after fire. *Forest Ecology and Management*, *147*, 67–74.

Dobson, M. C., Pierce, L., Sarabandi, K., Ulaby, F. T., & Sharik, T. (1992a). Preliminary analysis of ERS-1 SAR for forest ecosystem studies. *IEEE Transactions on Geoscience and Remote Sensing*, *30*, 203–211.

Dobson, M. C., Ulaby, T., Le Toan, T., Beaudoin, A., & Kasischke, E. S. (1992b). Dependence of radar backscatter on coniferous forest biomass. *IEEE Transactions on Geoscience and Remote Sensing*, *30*, 412–415.

Games, P. A., & Howel, J. F. (1976). Pairwise multiple comparison procedures with unequal N's and/or variances: A Monte Carlo study. *Journal of Education and Behavioral Statistics*, *1*, 113–125.

Goetz, S. J., Sun, M., Baccini, A., & Beck, P. S. A. (2010). Synergistic use of spaceborne lidar and optical imagery for assessing forest disturbance: An Alaska case study. *Journal of Geophysical Research*, *115*, 1–14.

Henry, M. C., & Hope, A. S. (1998). Monitoring post-burn recovery of chaparral vegetation in southern California using multi-temporal satellite data. *International Journal of Remote Sensing*, *19*, 3097–3107.

Hu, F. S., Brubaker, L. B., Gavin, D. G., Higuera, P. E., Lynch, J. A., Rupp, T. S., et al. (2006). How climate and vegetation influence the fire regime of the Alaskan boreal biome: The holocene perspective. *Mitigation and Adaptation Strategies for Global Change*, *11*, 829–846.

Imhoff, M. L. (1995). Radar backscatter and biomass saturation: Ramifications for global biomass inventory. *IEEE Transactions on Geoscience and Remote Sensing*, *33*, 511–518.

Kasischke, E. S., & Johnstone, J. F. (2005). Variation in post-fire organic layer thickness in a black spruce forest complex in Interior Alaska and its effects on soil temperature and moisture. *Canadian Journal of Remote Sensing*, *35*, 2164–2177.

Kasischke, E. S., Tanase, M. A., Bourgeau-Chavez, L. L., & Borr, M. (2011). Soil moisture limitations on monitoring boreal forest regrowth using spaceborne L-band SAR data. *Remote Sensing of Environment*, *115*, 227–232.

Kasischke, E. S., Williams, D., & Barry, D. (2002). Analysis of the patterns of large fires in the boreal forest region of Alaska. *International Journal of Wildland Fire*, *11*, 131–144.

Liew, S. C., Kwoh, L. K., Padmanabhan, K., Lim, O. K., & Lim, H. (1999). Delineating land/forest fire burnt scars with ERS Interferometric Synthetic Aperture Radar. *Geophysical Research Letters*, *26*, 2409–2412.

Marchetti, M., Ricotta, C., & Volpe, F. (1995). A qualitative approach to the mapping of postfire regrowth in Mediterranean vegetation with Landsat-TM. *International Journal of Remote Sensing*, *16*, 2487–2494.

Minchella, A., Del Frate, F., Capogna, F., Anselmi, S., & Manes, F. (2009). Use of multitemporal SAR data for monitoring vegetation recovery of Mediterranean burned areas. *Remote Sensing of Environment*, *113*, 588–597.

Notivol, E., Cabanillas, A., González, R., & Revuelta, C. (2005). Caracterización de masas naturales de pino carrasco (*Pinus halepensis* Mill.) en la depresión del Ebro. *IV Congreso Forestal Español* (pp. 299). Zaragoza: Sociedad Española de Ciencias Forestales.

Patterson, M. W., & Yool, S. R. (1998). Mapping fire-induced vegetation mortality using Landsat Thematic Mapper data: A comparison of linear transformation techniques. *Remote Sensing of Environment*, *65*, 132–142.

Pausas, J. G., Gimeno, T., & Vallejo, R. (Eds.). (2002). *Fire severity and pine regeneration in the eastern Iberian Peninsula*. Rotterdam: Millpres.

Pérez-Cabello, F. (2002). *Paisajes forestales y fuego en el Prepirineo occidental oscense. Un modelo regional de reconstrucción ambiental. Zaragoza.* Zaragoza.

Richards, J. A., Sun, G. -Q., & Simonett, D. S. (1987). L-Band radar backscatter modeling of forest stands. *IEEE Transactions on Geoscience and Remote Sensing*, *4*, 487–498.

Rignot, E. J., Williams, C. L., Way, J., & Viereck, L. A. (1994). Mapping of forest types in Alaskan boreal forests using SAR imagery. *IEEE Transactions on Geoscience and Remote Sensing*, *32*, 1051–1059.

Rouse, J. W., Haas, R. H., Schell, J. A., & Deering, D. W. (1973). Monitoring vegetation systems in the Great Plains with ERTS. *Third ERTS Symposium* (pp. 309–317)..

Ruecker, G., & Siegert, F. (2000). Burn scar mapping and fire damage assessment using ERS-2 Sar images in East Kalimantan, Indonesia. *International Archives of Photogrammetry and Remote Sensing*, *33*, 1286–1293.

Santoro, M., Fransson, J. E. S., Eriksson, L. E. B., Magnusson, M., Ulander, L. M. H., & Olsson, H. (2009). Signatures of ALOS PALSAR L-band backscatter in Swedish forest. *IEEE Transactions on Geoscience and Remote Sensing*, *47*, 4001–4019.

Siegert, F., & Ruecker, G. (2000). Use of multitemporal ERS-2 SAR images for identification of burned scars in south-east Asian tropical rainforest. *International Journal of Remote Sensing*, *21*, 831–837.

Sun, G. Q., Rocchio, L., Masek, J., Williams, D., & Ranson, K. J. (2002). Characterization of forest recovery from fire using Landsat and SAR data. *Geoscience and Remote Sensing Symposium, 2002. IGARSS '02. Proceedings. 2002 IEEE International* (pp. 1076–1078). Toronto, Canada.

Please cite this article as: Tanase, M., et al., Sensitivity of SAR data to post-fire forest regrowth in Mediterranean and boreal forests, *Remote Sensing of Environment* (2011), doi:10.1016/j.rse.2011.04.009

Takeuchi, S., & Yamada, S. (2002). Monitoring of forest fire damage by using JERS-1 InSAR. *Geoscience and Remote Sensing Symposium, 2002. IGARSS '02. Proceedings. 2002 IEEE International* (pp. 3290–3292). Toronto, Canada.

Tanase, M. A., Pérez-Cabello, F., Riva, J. d. l., & Santoro, M. (2010a). TerraSAR-X data for burn severity evaluation in Mediterranean forests on sloped terrain. *IEEE Transactions on Geoscience and Remote Sensing*, *48*, 917–929.

Tanase, M. A., Riva, J. d. l., Santoro, M., Toan, T. L., & Perez-Cabello, F. (2010b). Sensitivity of X-, C- and L-band SAR backscatter to fire severity in Mediterranean pine forests. *IEEE Transactions on Geoscience and Remote Sensing*, *48*, 3663–3675.

Tanase, M. A., Santoro, M., Riva, J. d. l., & Pérez-Cabello, F. (2009). Backscatter properties of multitemporal TerraSAR-X data and the effects of influencing factors on burn severity evaluation, in a Mediterranean pine forest. *Geoscience and Remote Sensing Symposium, 2009. IGARSS '09. 2009 IEEE International* (pp. 593–596). Cape Town, South Africa.

Tanase, M. A., Santoro, M., Wegmüller, U., Riva, J. d. l., & Perez-Cabello, F. (2010c). Properties of X-, C- and L-band repeat-pass interferometric SAR coherence in Mediterranean pine forests affected by fires. *Remote Sensing of Environment*, *114*, 2182–2194.

Tapias, R., Gil, L., & Fuentes-Utrilla, P. (2001). Canopy seed banks in Mediterranean pines of southeastern Spain: A comparison between *Pinus halepensis* Mill., *P. pinaster* Ait., *P. nigra* Arn. and *P. pinea* L. *Journal of Ecology*, *89*, 629–638.

Thiel, C. J., Thiel, C., & Schmullius, C. C. (2009). Operational large-area forest monitoring in Siberia using ALOS PALSAR summer intensities and winter coherence. *IEEE Transactions on Geoscience and Remote Sensing*, *47*, 3993–4000.

Toan, T. L., Beaudoin, A., & Guyon, D. (1992). Relating forest biomass to SAR data. *IEEE Transactions on Geoscience and Remote Sensing*, *30*, 403–411.

Ulander, L. M. H. (1996). Radiometric slope correction of synthetic-aperture radar images. *IEEE Transactions on Geoscience and Remote Sensing*, *34*, 1115–1122.

Viedma, Melia, J., Segarra, D., & Garcia-Haro, J. (1997). Modeling rates of ecosystem recovery after fires by using Landsat TM data. *Remote Sensing of Environment*, *61*, 383–398.

Viereck, L. A., Dyrness, C. T., Van Cleve, K., & Foote, M. J. (1983). Vegetation, soils, and forest productivity in selected forest types in interior Alaska. *Canadian Journal of Remote Sensing*, *13*, 703–720.

Vila, J. P. S., & Barbosa, P. (2010). Post-fire vegetation regrowth detection in the Deiva Marina region (Liguria-Italy) using Landsat TM and ETM+ data. *Ecological Modelling*, *221*, 75–84.

Wang, Q., Adiku, S., Tenhunen, J., & Granier, A. (2005). On the relationship of NDVI with leaf area index in a deciduous forest site. *Remote Sensing of Environment*, *94*, 244–255.

Wegmuller, U., & Werner, C. L. (1995). SAR interferometric signatures of forest. *IEEE Transactions on Geoscience and Remote Sensing*, *33*, 1153–1161.

Please cite this article as: Tanase, M., et al., Sensitivity of SAR data to post-fire forest regrowth in Mediterranean and boreal forests, *Remote Sensing of Environment* (2011), doi:10.1016/j.rse.2011.04.009